Forearm Impactor Tests for Development of Injury Risk Assessment Capability

Bengt Pipkorn, Jason Forman, Magnus Björklund, Joakim Risberg, Lotta Jakobsson

Abstract The forearm is one of the most injured body regions. To enable injury risk assessment a component test method using a novel instrumented forearm impactor was proposed. Impact tests with the forearm were carried out replicating published human subject impact tests. The forearm impactor elbow was mounted to a force transducer and a reaction plate assembly free to move along linear guide rails. The impact load was provided by a guided mass dropped from various heights. The drop heights were selected to generate elbow plate forces including both fractures and no fractures in the published tests. Tests were run with two boundary conditions.

The peak elbow plate forces ranged from 1.6 kN to 8.6 kN. The peak axial forces in the internal forearm loadcell varied from 1.9 kN to 9.7 kN. A linear relationship was defined between the forces recorded in the two loadcells for each boundary condition.

The linear relationship was developed to aid in translating the published forearm fracture risk curve to facilitate in predicting forearm fracture risk with the forearm impactor in axial impacts with an outstretched hand. The novel instrumented forearm impactor in combination with the injury prediction capability can be used to evaluate forearm fracture risk in hand impacts.

Keywords Forearm, Impactor, Radius, Ulna, Fracture.

I. INTRODUCTION

Automobile safety has undergone substantial improvements in the last few decades, resulting in reduced injury risk for all occupants in all crashes [1-2]. Belted occupants in newer model year vehicles (model year 2009 and later) generally have a lower risk of injury (AIS2+) than occupants in older model year vehicles [2]. However, forearm and hand or wrist injuries were found to be one of the most frequently injured (AIS2+) body parts for belted occupants in frontal impacts in newer model year vehicles [2]. In another study, seat-belt-induced clavicle fractures were found to be the most frequent, followed by wrist and forearm fractures [3]. For drivers in frontal impacts, fractures to the forearm, wrist, hand and clavicula were identified as the main upper extremity injuries [4]. Some of the main injury mechanisms were identified as impact to an outstretched, extended or clenched hand [4]. However, drivers and passengers were found to have different upper extremity injury patterns and the direction of impact influenced the injury pattern [5]. The front vehicle interior was identified as the most common injury source for forearm fractures [5]. For belted drivers, two different injury mechanisms for fractures to the upper extremities were described [6]. One was frontal crashes with direct impact to the vehicle interior with longitudinal and rotational load to hand, hand joint and forearm resulting in forward movement of the forearm and rotational effect, resulting in injury risk to joints and lower forearms. The other was side impacts with load transmission to lateral parts of the forearm resulting in injuries to the whole upper extremity. Upper extremity injury risk from airbag inflation was investigated in a study based on National Automotive Sampling System (NASS) database files from 1993 to 2000 [7]. The study included 2,413,247 vehicle occupants who were exposed to airbag deployment in the United States. It was found that airbag-induced injuries were elbow joint dislocations and forearm fractures.

Although usually not life-threatening, upper extremity injuries can lead to long-term consequences, influencing the daily life for these victims to different degrees and durations. Long-term consequences from a vehicle crash are an important component of the societal burden of motor vehicle crashes. In addition to reducing

B. Pipkorn (e-mail: bengt.pipkorn@autoliv.com; tel: +46 (0)322 626341) is Adjunct Professor at Chalmers University of Technology, Gothenburg, and Director of Simulation and Active Structures at Autoliv Research, Vårgårda, Sweden. J. Forman is a Principal Scientist, at the Center for Applied Biomechanics in the Department of Mechanical and Aerospace Engineering, University of Virginia, USA. M. Björklund is a Safety Architect, J. Risberg is a Senior Measurement Engineer, and L. Jakobsson is Senior Technical Leader, Injury Prevention at Volvo Cars Safety Centre, Volvo Cars, Sweden. L. Jakobsson is also Adjunct Professor in Vehicle Safety at Chalmers.

the quality of life for the victims, they are very costly for society [8]. Long-term consequences for upper extremity injuries were seen irrespectively of crash configuration, with PMI1+ ranging between 14.5-30.0%. Wraighte et al. [9] calculated financial costs and functional impairment of upper extremity injuries to 62 front seat occupants in frontal impacts in the UK, showing the highest average upper extremity impairment to the elbow and wrist.

The fracture tolerance of forearm and wrist was evaluated by Forman *et al.* [10]. Fifteen forearm axial impact tests with extended hand were carried out. It was found that an axial reaction force of 4.3 kN in the elbow corresponded to a 50% fracture risk of the forearm. Duma *et al*. [11] carried out 17 impact tests with a free hanging forearm. The impacted forces ranged from 1.7 kN to 4.7 kN. Fractures were obtained in radius, ulna, scaphoid and lunate. Three point bending tests with 10 pairs of human cadaveric lower arm specimens were carried out [12]. Either the radius or ulna was impacted quasi-statically or dynamically. Fractured occurred close to the loading site with a peak average load of 1370N and a peak average moment of 89 Nm. It was also found that the difference between radius and ulna fracture load was not significant. 1213A component test method can be a practical method for addressing the variety of hand impacts to vehicle interior, such as instrument panel and door trim, to help in evaluation and development of safety systems. There are few methods and tools addressing the mechanism of hand and forearm injuries in vehicle safety testing. The Research forearm Injury Device (RAID) [14], a small female-sized Hybrid-III forearm [15] and a midsize male forearm [13] were designed for evaluation of airbag interactions. An instrumented forearm was also developed and used in a side airbag out-of-position test method [16]. These tools are not intended to be used for direct impact to interior vehicle surfaces. A novel instrumented forearm was developed for impact testing to enable evaluation of fracture risk to the wrist and distal part of the ulna and radius [17]. The instrumented forearm was developed by in house modifications of a midsize male Hybrid-III crash test dummy forearm. Modification details can be found in [17]. The instrumented forearm can be used as a free-flying impactor as well as mounted on a crash test dummy. None of these tools is included in standardized testing, except for the tool used in the out-of-position test method. In addition, the novel instrumented forearm has limited capability to predict fracture risk due to lack of risk curves.

With the overall purpose of developing injury risk assessment for the novel instrumented forearm impactor, the objective of this study is to recreate published human subject tests with the forearm impactor and arrive at a force relationship for which the internal load cell can relate to the published injury risk curves. Specifically, the objective is to develop a linear relationship (transfer function) between the forearm impactor axial force (arm Fz) and the elbow plate reaction force (elbow Fz) in the test rig used, for two elbow boundary conditions.

II. METHODS

The novel instrumented forearm impactor based on a midsize male Hybrid-III forearm was used (Fig. 1) [17]. The forearm impactor is instrumented with three sensors that capture force, acceleration and bending moment. Force is measured using a six-axis force transducer sensor in the middle section of the steel bar representing the long bones, ulna and radius. This study focused on the axial force in the forearm (arm Fz).

Six axis force transducer

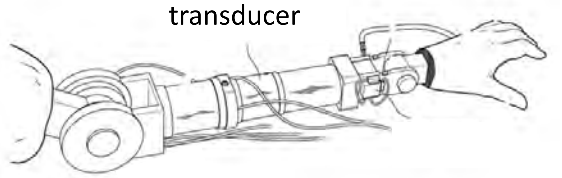

Fig. 1. Novel Instrumented Forearm.

Impact tests were carried out with the forearm impactor, replicating published human subject impact tests [10]. The same setup was used, including a drop tower test rig (Fig. 2). The impact load was provided by a guided mass (''hammer'') dropped from various heights (Fig. 2). The forearm impactor was mounted into the fixture by attaching the proximal boundary of the arm (elbow) to a guided reaction plate (elbow plate). The distal end of the arm (the hand) was positioned with the wrist extended to approximately 90 degrees and slightly preloaded by a guided contact plate assembly supported by the hand (Fig. 2). The forearm impactor was oriented such that the long axis was aligned with the velocity vector of the hammer. For each test, the hammer (32 kg mass) was dropped from various heights above the point of first contact with the impact plate assembly, achieving variable velocity. The various heights were selected to achieve impact velocities that generated elbow forces that covered the range from no fractures to fractures in the corresponding published human subject tests [10]. Impacting force was transferred from the impactor to the forearm impactor via a load transfer plate assembly. Aluminium honeycomb was placed between the hammer and the impact plate assembly to control the forces generated and to avoid metal-to-metal contact. The hammer impact plate assembly and the elbow plate were all mounted on linear guide rails to prevent off-axis motion.

In total, 19 tests were carried out with the forearm impactor, in which the boundary conditions and the drop height were varied. Two different boundary conditions were included: 'fixed elbow' and 'free elbow'. In the 'fixed elbow' condition, the elbow plate was rigidly fixed to the base of the test device. In the 'free elbow' condition, the elbow plate was free to move along the linear guide rails, with the elbow reaction forces (elbow Fz) generated by the inertia of the elbow-mounting assembly. This condition was used to simulate inertial loading that may occur at the elbow when an impact load is applied to an outstretched hand to arrest motion of the body. The total mass of the elbow reaction assembly (potting cup, load cell, elbow plate) was 8.5 kg. In this condition, the elbow plate was initially positioned above the base of the drop tower using breakaway polystyrene blocks, which released at the initiation of testing, allowing the elbow reaction assembly to move under its own inertia. At hammer impact to the contact plate assembly the velocity of the elbow plate was 0 m/s. Blocks of foam were placed 15.2 cm below the elbow assembly to arrest the motion of the forearm impactor at the conclusion of the tests. The post-contact stroke of the hammer was limited via mechanical stops to prevent secondary impact upon deceleration of the forearm impactor.

The elbow plate reaction forces were measured with a six-axis load cell (Model 3868TF, Humanetics, Plymouth, MI). In the 'free elbow' boundary conditions, acceleration of the elbow plate was measured with an uniaxial accelerometer (Model 7264B-2k, Endevco, Irvine, CA). The acceleration was used to compensate the force readings for the inertia of the moving elbow plate for the 'free elbow' boundary condition. This allowed the calculation of the force applied to the elbow boundary of the test object by the elbow plate reaction force. The forearm impactor force was measured with a six-axis load cell (Denton 2432).

Transfer functions were developed as linear relationships comparing the forearm impactor's axial force (arm Fz) and the corresponding peak elbow plate reaction force (elbow Fz) on the test rig. All data (forces and acceleration) were collected at 10,000 samples per second using a high-speed digital data acquisition system (DEWE-2010 Series, Dewetron, Graz, Austria). The elbow plate reaction force (elbow Fz) was inertially compensated, and thereafter the compensated elbow reaction and the forearm impactor forces (arm Fz) were digitally filtered using a Channel Filter Class (CFC) 600 filter.

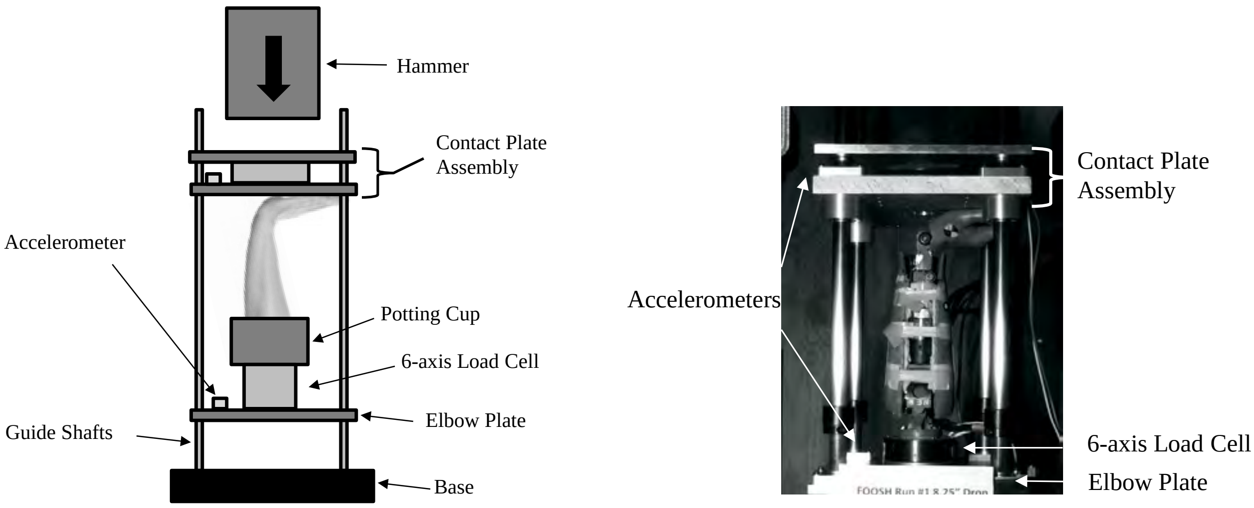

Fig. 2. The test rig setup. The elbow-mounting assembly was free to move in the direction of impact under its own inertia on a set of guiding rails. The human subject test in [10] (left) and the forearm impactor in the current study (right).

III. RESULTS

For the tests with 'free elbow' boundary conditions, the different dropping heights resulted in impact velocities between 1.68 m/s and 5.33 m/s (Table I). The force plots are shown in Appendix A, and peak forces in Table I. The peak forearm impactor's axial force (arm Fz) ranged from 1.9 kN to 9.7 kN. The corresponding peak elbow Fz ranged from 1.6 kN to 8.6 kN. The arm Fz was consistently higher than the elbow Fz.

TABLE I
IMPACT VELOCITY AND PEAK FORCES IN THE TESTS WITH 'FREE ELBOW' BOUNDARY CONDITION

Test Nr	A1	A2	A3	A4	A5	A6	A7	A8	A9	A10
Velocity (m/s)	1.76	1.79	1.74	1.68	3.77	3.77	3.77	5.33	5.26	5.12
Peak arm Fz (N)	1893	2321	2351	2346	5721	6203	6214	8863	9658	8766
Peak elbow Fz (N)	1585	2102	2101	2048	4947	5457	5496	7805	8600	7729

A linear relationship of y=0.88x (R^2=0.999) was obtained for elbow Fz and arm Fz in the 'free elbow' boundary condition (Fig. 3).

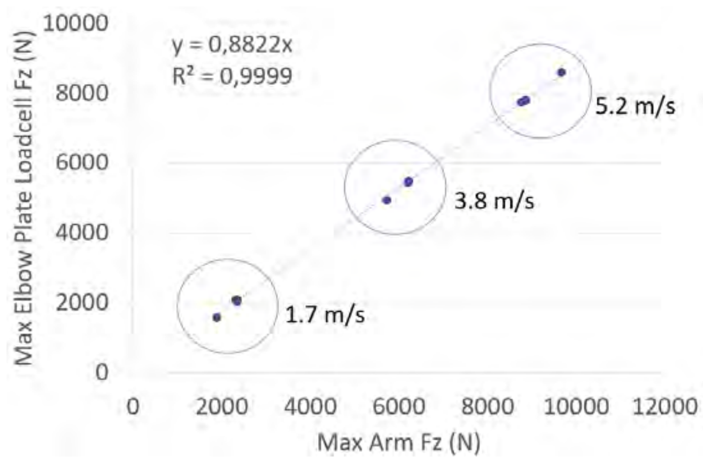

Fig. 3. Transfer functions based on relationship of peak arm Fz and peak elbow plate Fz for tests with 'free elbow' boundary condition.

For the impact tests with 'fixed elbow' boundary conditions, the different dropping heights resulted in impact velocities between 1.60 m/s and 3.95 m/s (Table II). The force plots are shown in Appendix B, and peak forces in Table II. The peak forearm impactor's axial force (arm Fz) ranged from 4.2 kN to 10.8 kN. The corresponding peak elbow Fz ranged from 4.3 kN to 11.1 kN. Peak arm Fz was lower than peak elbow Fz for all but three tests.

TABLE II
IMPACT VELOCITY AND PEAK FORCES IN THE TESTS WITH 'FIXED ELBOW' BOUNDARY CONDITION

Test Nr	B1	B2	B3	B4	B5	B6	B7	B8	B9
Velocity (m/s	1.62	1.60	1.92	1.73	1.85	3.73	3.70	3.95	3.80
Peak Arm Force (N)	4200	7462	4413	6480	5534	9855	9692	7283	10786
Peak Elbow Force (N)	4282	7410	4380	6404	5554	10168	10184	7941	11131

A linear relationship, y=1.03x (R^2=0.999), was obtained for elbow Fz and arm Fz in the 'fixed elbow' boundary condition (Fig. 4).

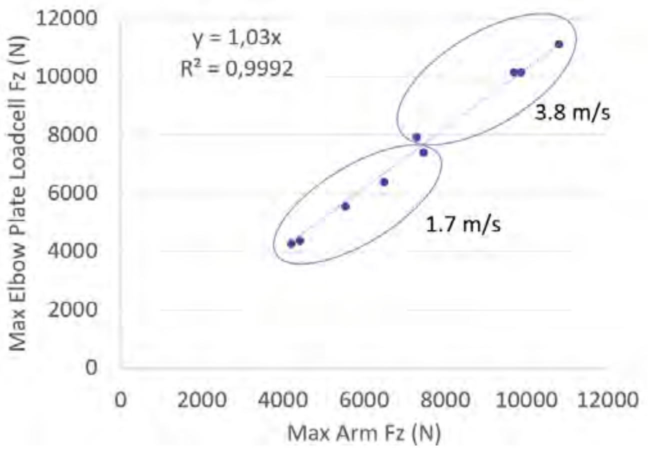

Fig. 4. Transfer functions based on relationship of peak arm Fz and peak elbow plate Fz for tests with 'fixed elbow' boundary condition.

IV. DISCUSSION

With the goal of enabling prediction of forearm fracture risk in axial impacts, tests with an instrumented forearm impactor were carried out In the test a hammer was dropped from various heights, producing impact energies (velocities) on the forearm impactor in the range from non-injurious to injurious impacts. Force was recorded in the forearm impactor and the elbow plate of the test rig. In the tests with the 'free elbow' conditions differences in peak load in tests with the same impact velocity and the same boundary conditions was obtained. The reason for the differences can be due to the tolerances of the aluminum honeycomb that was placed between the hammer and the contact plate assembly to control the forces generated and to avoid metal-to-metal contact. In the tests with the 'fixed elbow' condition despite the fact that the forearm impactor was oriented such that the long axis was aligned with the velocity vector of the hammer various degrees of small flexion of the forearm impactor was observed resulting in differences in peak load. However, the goal with the study was to quantify the relationship between the external forces and the forearm loadcell forces, for which the data was very consistent regardless of some variability in the input forces.

In the testing carried out by Forman et al. [10] the range of elbow plate forces were for the 'free elbow' boundary condition between 3.3 to 5.0kN. Injuries were obtained for forces as low as 3.3kN. The fractures were to the radius, ulna, scapula and triquetrum. For the 'fixed elbow' boundary condition the range of elbow plate forces were 4.9 to 5.4kN and the fractures obtained were to the radius, ulna, scaphoid, lunate, and triquetrum.

Linear transfer functions were developed to enable translation of the forearm impactor force to the elbow plate reaction force. Based on the results from the testing by Forman et al. [10] one risk curve was proposed to predict fracture risk for both the 'free elbow' and the 'fixed elbow' conditions (Fig. 5.). The linear transfer functions can be used with the risk curve to predict the risk for radius, ulna or wrist fracture for both the 'free elbow' and the 'fixed elbow' boundary conditions with the novel instrumented forearm impactor.

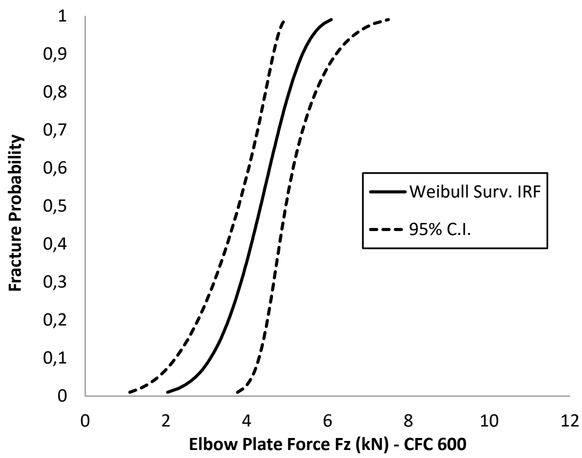

Fig. 5. Fracture risk function with elbow plate force as predictor variable from [10].

Forearm fracture risk from impact was also assessed in a study by Duma *et al*. [11]. It was found that a palm impact force of 1.7 kN corresponded to a 50% fracture risk of the wrists of 5th percentile female post-mortem human subjects (PMHS), while in the study by Forman *et al.* [10] a reaction force of 4.34 kN measured at the elbow corresponded to a 50% fracture risk of the radius, ulna and wrist. The tests were carried out with two boundary conditions and the forces were measured at different locations on the specimens. In the study carried out by Duma *et al*. [11], only female subjects were included. The forearm impactor in the current study corresponds to a mid-sized male. Therefore, the tests carried out by Forman *et al.* [10] were selected for development of injury risk assessment for the forearm impactor.

In a vehicle impact, the forearm fracture risk from impact to the vehicle interior depends on multiple factors, such as the impact locations and the boundary conditions of the forearm at impact. The boundary conditions are influenced by the crash configuration, the geometry and orientation of the arm, the pre-impact muscular bracing and the location of the arm in the crash (e.g., if the hand is positioned on the armrest). For the impact testing in the current study, two boundary conditions were selected: 'free' and 'fixed'. These boundary conditions were considered to cover the variety of boundary conditions for axial impacts of the forearm to the vehicle interior in vehicle impacts such as hand impacts to the instrument panel and pushing on to the steering wheel in frontal impact crashes. Future developments of the forearm impactor can include non-axial impact of the forearm. The 'free elbow' condition was used to mimic inertial loading that can occur at the elbow when an impact load is applied to an outstretched hand and arm to arrest motion of the forearm. The 'fixed elbow' condition can occur when there is a strong coupling between the upper body of the occupant and the arm when the forearm is impacting the vehicle interior.

The wrist of the instrumented forearm is a simple representation of the human wrist. However, in both the human subject tests and the tests with the instrumented forearm impactor, the forearms were oriented such that the long axis was aligned with the velocity vector of the hammer. The main load from the hammer was in the direction of the forearm. Therefore, the influence from the wrist on the forearm load was small.

Mitigating forearm fractures of vehicle occupants is challenging. Based on the large variety of occupant characteristics, sitting postures and crash configurations, the forearm trajectories, contact points and loading mechanism can vary substantially [9]. The transfer function developed in the current study, in combination with the corresponding fracture risk function from [10], takes one step towards predicting forearm fracture risk in hand impacts when using the forearm impactor. Following steps can include development of risk functions and injury assessment reference values (IARVs) to be used with the forearm impactor to predict fracture risk.

V. CONCLUSIONS

Linear transfer functions were developed that enabled translation of impact forces measured in the novel instrumented forearm impactor to elbow plate reaction forces. These transfer functions can be used in combination with a published risk curve, based on elbow place reaction forces, to predict radius, ulna and wrist fracture risks for axial impacts. By this means, the novel instrumented forearm impactor, in combination with the injury prediction capability, can be used to evaluate forearm fracture risk in axial impacts with outstretched hands.

VI. ACKNOWLEDGEMENTS

The project was carried out at SAFER – Vehicle and Traffic Safety Centre at Chalmers, Sweden, and financed by Strategic Vehicle Research and Innovation (FFI), by VINNOVA, the Swedish Transport Administration, the Swedish Energy Agency, and the Swedish vehicle industry. The authors would like to thank our peer researchers within the project, especially: Victor Alvarez, Svein Kleiven, Madelen Fahlstedt and Helena Stigson.

VII. REFERENCES

[1] Klinich, K. D., Bowman, P., Flannagan, C. A., Rupp, J. D. (2016) University of Michigan Transportation Research Institute (UMTRI). Injury patterns in motor-vehicle crashes in the United States: 1998-2014, Ann Arbor, MI, USA.

[2] Forman, J., Poplin, G. S., *et al*. (2019) Automobile injury trends in the contemporary fleet: Belted occupants in frontal collisions. *Traffic Injury Prevention*, **20**(6): pp.607–612.

[3] Chung, K. C., Spilson, S. V. (2001). The frequency and epidemiology of hand and forearm fractures in the United States. *Journal of Hand Surgery (American Volume)*, **26**(Suppl 5): 908Y915.

[4] Jakobsson, L., Lindman, M. (2010). Upper extremity fractures in car accidents. *Proceedings of IRCOBI Conference*, 2010, Hannover, Germany.

[5] Conroy, C., Schwartz, A., *et al*. (2007) Upper extremity fracture patterns following motor vehicle crashes differ for drivers and passengers. *International Journal of the Care of the Injured*, **38**: pp.350–357.

[6] Otte, D. (1998) Biomechanics of upper limb injuries of belted car drivers and assessment of avoidance. *Proceedings of IRCOBI Conference*, 1998, Gothenburg, Sweden.

[7] Jernigan, V., Rath, A., Duma, S. (2005) Severe upper extremity injuries in frontal automobile crashes: The effects of depowered airbags. *The American Journal of Emergency Medicine*, **32**: pp.99–105.

[8] Malm, S., Krafft, M., Kullgren, A., Ydenius, A., Tingvall, C. (2008) Risk of Permanent Medical Impairment (RPMI) in Road Traffic Accidents. *Proceedings of 52nd AAAM Annual Conference Annals of Advances in Automotive Medicine.*

[9] Wraighte, P. J., Manning, G., Wallace, W. A. and Hynd, D. (2007) Upper extremity injuries in road traffic accidents. *ESV Conference*, Paper No. 07-0239, 2007, Lyon, France.

[10] Forman, J., Perry, B., *et al*. (2014) Injury tolerance of the wrist and distal forearm to impact loading onto outstretched hands. *The Journal of Trauma Acute Care Surgery*, **77**(3 Suppl 2): pp.176–183.

[11] Duma, S. M., Boggess, B. M., Crandall, J. R., MacMahon, C. B. (2003) Injury risk function for the small female wrist in axial loading. *Accident Analysis & Prevention*, **35**(Suppl 6): 869Y875.

[12] Begeman, P. C., Pratima, K., Prasad, P. (1999) Bending strength of the human cadaveric forearm due to lateral loads. *Proceedings of 43rd Stapp Car Crash Conference*, SAE-99SC24, 1999, San Diego, California, USA.

[13] Saul, R., Backaitis, S., Beebe, M. and Ore, L. (1996) Hybrid III dummy instrumentation and assessment of forearm injuries during air bag deployment. *Proceedings of 40th Stapp Car Crash Conference*, SAE- 962417, 1996, Albuquerque, New Mexico, USA.

[14] Kuppa, S., Olson, M., *et al*. (1997) RAID - An investigative tool to study air bag/upper extremity interactions. SAE Technical Paper 970399, 1997, Detroit, Michigan, USA.

[15] SAE International (2017) SAE Instrumented forearm User's Manual, USA.

[16] Lund, A. K. (2003) The Side Airbag Out-of-Position Injury Technical Working Group (A joint project of Alliance, AIAM, AORC, and IIHS). Recommended procedures for evaluating occupant injury risk from deploying side airbags – First Revision. USA.

[17] Björklund, M., Risberg, J., Laudon, O., Jakobsson, L. (2020) Development of a Hand and Forearm Impact Test Method and a Study on Influencing Factors. *Proceedings of IRCOBI Conference*, 2020, Virtual.

VIII. APPENDIX

A. 'Free Elbow' Boundary Condition Force Plots

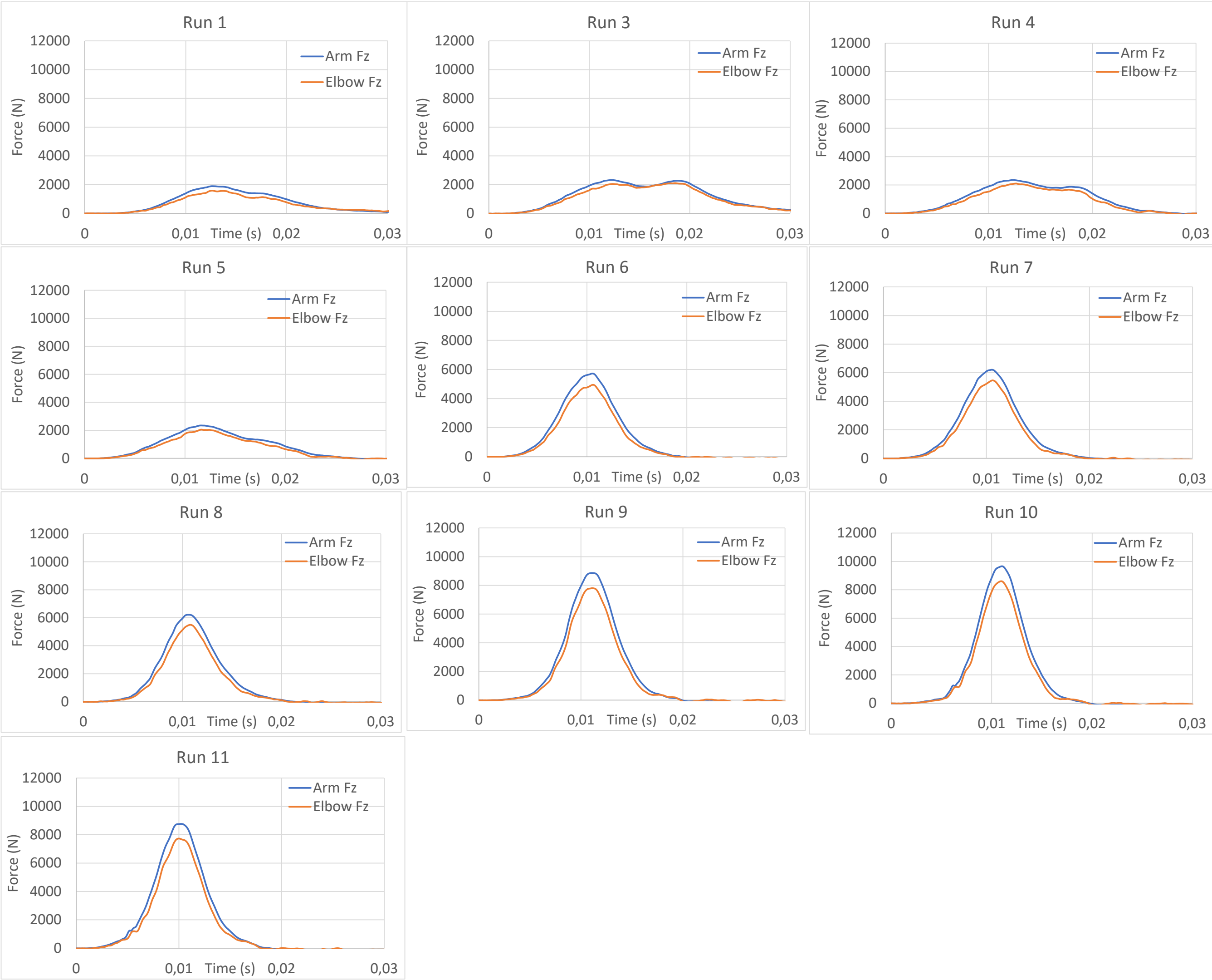

B. 'Fixed Elbow' Boundary Condition Force Plots